

CHAPTER TWENTY SEVEN

WAVE COHERENCE IN COASTAL WATERS

Steven A. Hughes* , M.ASCE

ABSTRACT: The spatial variability of the near-shore wave field is examined in terms of the coherence functions found between five closely spaced wave gages moored off the North Carolina coast in 17 meters depth. Coherence was found to rapidly decrease as the separation distance increased, particularly in the along-crest direction. This effect is expressed as nondimensional coherence contours which can be used to provide an estimate of the wave coherence expected between two spatial positions.

INTRODUCTION

The coherence function between two spatially separated time series of ocean waves measures the extent to which the waves occurring at one position can be predicted from the wave field at the other position, assuming a linear dependence exists between the wave time histories at the two locations. The coherence function rapidly decreases as the distance between the two spatial positions increases. This decrease arises because most naturally occurring waves are not long-crested and the waves change form as they propagate. Ocean waves are conveniently described in terms of energy spectra, with empirically determined parameters relating the spectra between locations. In many applications a spectral representation of the wave field is sufficient, however, there are instances when it would be useful to estimate the wave coherence function between two positions. A case in point is an investigation by the Naval Civil Engineering Laboratory (NCEL) into ship motions and mooring forces for vessels anchored in coastal waters.

A mooring forces numerical model has been developed by the NCEL which simulates ship motions and resultant mooring loads under various mooring configurations and wave conditions, but field data are needed to verify the model's accuracy and to determine its limits of applicability. In the NCEL numerical model the wave field is to be applied at the ship's center of gravity. Since waves cannot be measured at this position, it is necessary in the course of a

* Hydr. Engr., Coastal Engineering Research Center, U.S. Army Engineer Waterways Experiment Station, P.O. Box 631, Vicksburg, Mississippi 39180 USA.

field experiment to collect wave data a short distance away from the ship where the waves are free of excessive ship-induced interference. These waves, which are slightly different from those waves causing the ship motion, are used to drive the numerical model, producing a time history of the mooring loads.

Evaluation of the mathematical algorithms in the model can be performed by finding the coherence function between the measured ship response and the response predicted by the model. This response coherence is composed of the coherence due to the approximations made in the mathematical algorithms and the wave coherence between the position where the waves were measured and the ship's center of gravity. Therefore, it is necessary to either: 1) estimate or directly measure wave coherence as a function of spatial separation so that it may be factored out of the response coherence, or 2) position the wave gage in a location which helps maximize the wave coherence.

It was this application that prompted the NCEL to sponsor a month-long wave coherence experiment at the Coastal Engineering Research Center's Field Research Facility at Duck, North Carolina during the Spring of 1983. The primary objective of the experiment was to collect simultaneous wave data from an array of five closely spaced wave gages for events of wind seas, swell, and multi-directional wavetrains, and to then examine the spatial variability in the wave field. This paper presents the findings of the experiment.

DATA COLLECTION

Between April 23 and June 10, 1983, wave data were collected from an array of 5 Datawell Waverider wave gages moored in a depth of 17 meters. The array was positioned about 2 kilometers offshore of the Field Research Facility (FRF) at Duck, North Carolina (Fig. 1). The dimensions and orientation of the Waverider array, as shown in Fig. 2, were determined using a land-based laser surveying instrument during calm conditions after the array was installed. The local bottom slope in the area is on the order of 1:200, resulting in less than a meter difference in water depth over the site. All the buoys in the array were tethered to mooring lines of equal scope with the intent that any displacement due to a unidirectional current would result in a translation of the array with minimum distortion. There was some variation in the array dimensions and orientation due to wave induced excursions of the buoys, but these spatial differences are small compared to the dimensions of the array and should average out over the period of data collection.

Prior to deployment all the Waveriders were calibrated according to the manufacturer's recommendations using a ferris wheel arrangement, and all the gages met or exceeded the calibration specification required by Datawell. A check on two of the gages after the experiment indicated

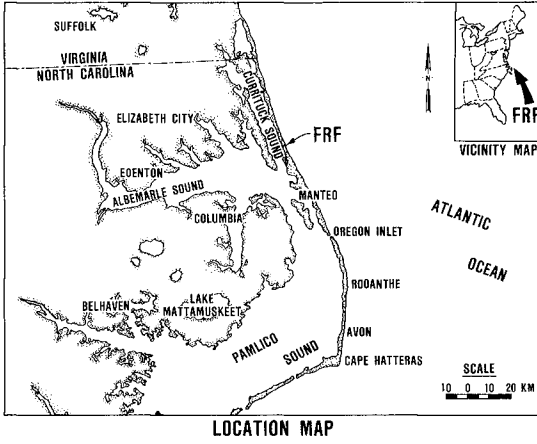


Figure 1. Field Research Facility Location Map

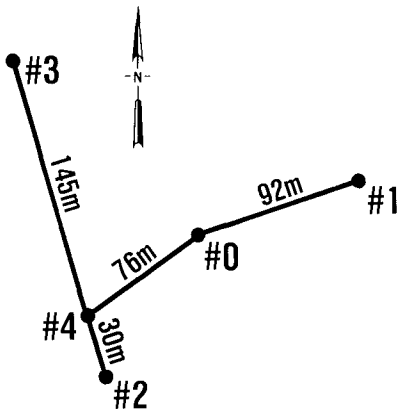


Figure 2. Waverider Wave Gage Array

that the calibration error for these two instruments was less than 4 percent.

The original data set is comprised of 38 data collection sessions lasting 80 minutes each. Each session involved the simultaneous recording of the wave height time series (as determined from buoy accelerations) from all gages at a sampling rate of 4 data points per second, resulting in a total record length of 19,200 data points per wave gage. The collection sessions were substantially longer than normal because it was realized that a fairly unique data set was being assembled and longer records might be of interest in future studies. The raw data were recorded by a digital computer and stored on magnetic tape.

The wave direction for each recording session was routinely obtained using an X-band imaging radar at the Field Research Facility, supplemented by visual observations. Mattie and Harris (5) report the direction measuring capability of the imaging radar to be accurate to within +4 degrees. During periods when two distinct wave trains were approaching from different directions, the direction of both the primary and secondary wave train was recorded. Pertinent weather data were noted during each recording session, and aerial photographs of the wave field were obtained several times over the duration of the experiment.

Realtime monitoring of the instruments during collection sessions helped insure that reasonable data were being obtained. Buoy number 2 (the buoy at the most southerly location on Fig. 2) produced erratic results from the onset of the experiment, and was replaced with a backup buoy as soon as possible. Consequently, the data from the first 22 collection sessions do not include results from this location. The 16 sessions after run number 22 include results from all locations in the array.

DATA ANALYSIS

Nine of the data collection sessions, representing a fairly broad range of conditions, were selected for detailed analysis (Table 1). For each selected data session the energy density spectrum for each gage was calculated and cross-spectral analysis was performed to determine the coherence and phase functions between all possible gage pairings. By definition the coherence function is given as

$$\gamma_{xy}(f) = \frac{|G_{xy}(f)|}{[G_{xx}(f) G_{yy}(f)]^{1/2}} \quad (1)$$

where

$G_{xx}(f)$ = autospectral density function of gage X,

$G_{yy}(f)$ = autospectral density function of gage Y, and

$G_{xy}(f)$ = cross-spectral density function between X and Y.

TABLE 1. Analyzed Data Set

Data Ref. No.	Date	H_{mo}^1 (m)	T_p^2 (sec)	Wave Direction ³ (degrees)	Ave. Wind Speed (m/s)	Ave. Wind Direction (degrees)
1	23 Apr	0.5	8.5	130/55 ⁴	4.0	133
2	23 Apr	0.8	3.6	127	10.0	142
3	24 Apr	2.5	9.3	125	6.7	203
4	24 Apr	1.6	9.5	125	7.0	225
5	25 Apr	1.1	10.5	45/125	7.5	290
6	17 May	2.0	7.0	55	12.0	32
7	17 May	1.3	6.5	55	7.0	32
8	19 May	1.1	5.5	110/80	5.0	146
9	10 Jun	1.9	6.5	80	9.4	34

- ¹ Significant wave height (four times the standard deviation of the sea surface elevations).
- ² Peak spectral wave period.
- ³ Direction from which waves are approaching.
0 -North; 90 -East; 180 -South; 270 -West.
- ⁴ Primary wave direction/Secondary wave direction (when two distinct wavetrains were present).

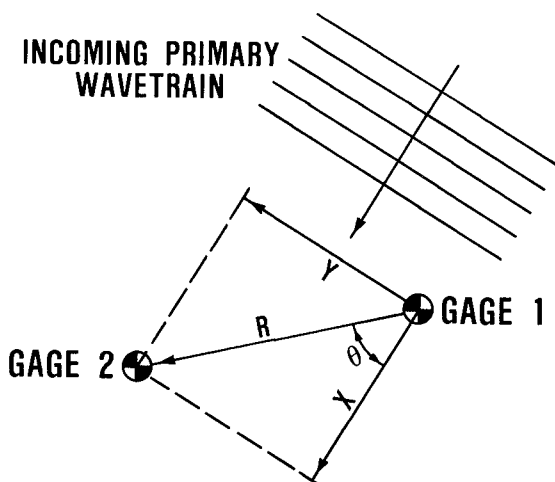


Figure 3. Reference Coordinate System

The coherence values are bounded between zero (no dependence) and one (complete linear dependence).

The data were processed with a fast Fourier transform routine using every other data point in the first 2048 seconds of the recorded time series. Thus the analysis subset contained 4096 points sampled at a 2 hertz rate (1/2 second interval). There is evidence that coherence estimates are not appreciably improved by increasing the length of the time series beyond 2048 data points (1). The resolution in the frequency domain is 0.0004883 hertz. Attention was concentrated on the frequency range 0- to 0.25-hertz since coherences at higher frequencies are expected to be quite small. Within this range spectral values are given at 512 discrete frequencies. A Tukey filter was applied to the cross-spectrum Fourier coefficients to increase the statistical stability of the results with only a minor loss in resolution. Coherence and phase were computed from the smoothed cross-spectral values.

Using the rather arbitrary criterion that coherence values greater than 0.7 indicate a meaningful coherence between gages, the results were examined, and it was found that about half (36) of the gage pairings had meaningful coherence in at least part of the frequency range. The autospectra and coherence functions for those gage pairings selected by this criterion are given in Hughes (3). The cases without meaningful coherences represented gage pairings with large spatial separation.

QUALITATIVE OBSERVATIONS

For each incident wave direction the distance vector separating any wave gage pairing can be resolved into a crest-parallel (along-crest) component, Y, and a crest-perpendicular (down-crest) component, X, as illustrated in Fig. 3. By comparing gage pairings with similar values for X and Y, several qualitative trends were observed. For example, Runs 3 and 7 (Fig. 4) and Run 6 (Fig. 5) have similar spatial separation for the selected gage pairings, and the coherence plots for these three runs are quite similar even though the autospectra differ considerably between runs. This comparison and other similar comparisons suggest that the coherence function is weakly, if at all, dependent upon the shape of the spectrum (compare Runs 3 and 7), the total energy contained in the spectrum, or the location of the spectral peak (compare Runs 3 and 6) for the range of conditions examined. Reasonably high coherence is observed at frequencies lower than the peak frequency so long as there is at least a small amount of energy present. The relatively high coherences at low frequencies could be attributed to the fact that waves at these frequencies are rendered less dispersive by the depth than waves at higher frequencies, and hence, can propagate with less alteration in form and celerity than higher frequency waves. These trends appear to be fairly consistent throughout the examined data. Run 5 (Fig. 5) was

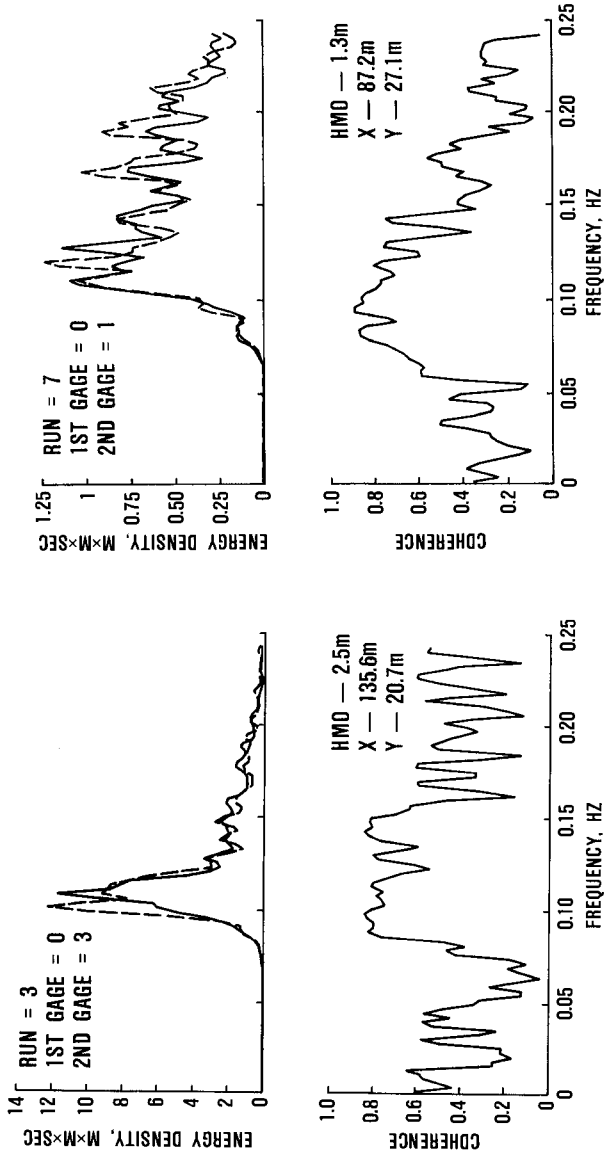


Figure 4. Comparison of Coherence Functions, Runs 3 and 7

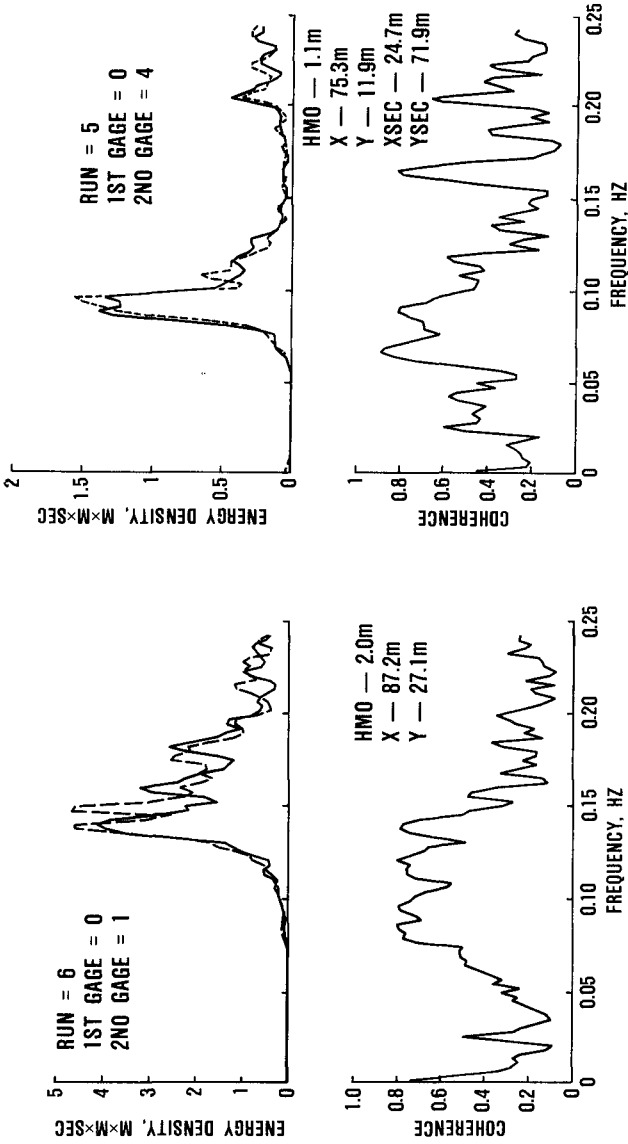


Figure 5. Comparison of Coherence Functions, Runs 6 and 5

included to illustrate the decrease in wave coherence caused by the visually observable presence of two wave trains propagating from different directions.

The most apparent influence on the wave coherence function is the spatial separation of the wave buoys. The observed trend is for a decrease in wave coherence, particularly at higher frequencies, as the spatial separation increases, and the trend is more evident with increases in along-crest separation than with down-crest separation. In other words the coherence found between gages separated by 30 meters in the down-crest direction will be somewhat better than the coherence between gages 30 meters apart in the along-crest direction.

WAVE COHERENCE CONTOURS

One of the goals of this study was to arrive at a method for estimating the wave coherence function in terms of the important parameters, which appear to be mainly frequency and spatial separation. A convenient way of incorporating frequency into the analysis was to nondimensionalize the along-crest (Y) and the down-crest (X) distances by the wavelength associated with each discrete frequency at the 17-meter water depth (linear theory). Then all discrete coherence values can be plotted against separation distances given in terms of relative wavelength. A survey of the discrete coherence values revealed that meaningful coherence values (greater than 0.7) were almost exclusively contained within the frequency range 0.08 - 0.16 hertz (wave periods 12.5 - 6.3 seconds). Since this frequency range covers the region where most coastal wave energy is concentrated, it was decided to limit the ensuing analysis to the discrete coherence values within this range.

Plotting of coherence values as a function of relative down-crest separation (X/L) and relative along-crest separation (Y/L) led to the subjective sketching of contours of equal coherence. These contours resembled those of an elliptic surface, suggesting that a satisfactory approximation might be obtained by the fitting of an elliptic surface to the data, i.e.,

$$\frac{(X/L)^2}{a^2} + \frac{(Y/L)^2}{b^2} = 1 \quad (2)$$

where a and b are some function of the wave coherence. Under the assumption that coherence decays exponentially as a function of the magnitude and direction of the vector separating the two positions, coherence can be expressed as

$$\gamma = e^{-f(R/L, \theta)} \quad (3)$$

where

$$\begin{aligned} \gamma &= \text{coherence,} \\ L &= \text{wavelength by linear theory,} \\ R &= (X^2 + Y^2)^{1/2}, \text{ and} \\ \theta &= \arctan (Y/X) \end{aligned} \quad (4)$$

The cylindrical coordinate system (Eqs. 4 and 5) is oriented so that the down-crest direction (X/L) corresponds to 0 degrees and the Y/L axis aligns with 90 degrees.

Transforming Eq. 2 into cylindrical coordinates and taking the square root of both sides yields

$$\frac{R}{L} \left[\frac{\cos^2 \theta}{a^2} + \frac{\sin^2 \theta}{b^2} \right]^{1/2} = 1 \quad (6)$$

Taking the logarithm of Eq. 3 and rearranging gives

$$\frac{f(R/L, \theta)}{-\ln(\gamma)} = 1 \quad (7)$$

By equating Eqs. 6 and 7, it is seen that one expression for the unknown function, f , is

$$f(R/L, \theta) = \frac{R}{L} [(c \cos \theta)^2 + (d \sin \theta)^2]^{1/2} \quad (8)$$

where

$$c = \frac{-\ln(\gamma)}{a} \quad \text{and} \quad d = \frac{-\ln(\gamma)}{b} \quad (9)$$

and c and d are the constants to be determined from the coherence data.

After discarding coherence values less than 0.5, the remaining 4000 discrete values of coherence as a function of X/L and Y/L were used to determine the values of c and d which minimized the sum of the square of the errors between the observed and predicted coherence values. The data collected when multiple wave trains were approaching from different directions were not included in this formulation. The resulting "best-fit" equation is

$$\gamma = \exp\left\{-\frac{R}{L} [(0.18 \cos \theta)^2 + (0.39 \sin \theta)^2]^{1/2}\right\} \quad (10a)$$

or in rectangular coordinates,

$$\gamma = \exp\left\{-[(0.18 X/L)^2 + (0.39 Y/L)^2]^{1/2}\right\} \quad (10b)$$

There are certainly a multitude of other surfaces which could be fit to the data with equal or slightly better success, but the present solution offers reasonable simplicity. As an indication of the scatter present in the data, the root-mean-square error between the measured coherence and that predicted by Eq. 10 was calculated and found to be 0.126, which is quite large.

The coherence contours found from Eq. 10 are presented in Fig. 6 as a function of nondimensional along-crest separation distance (horizontal axis) and nondimensional down-crest separation distance (vertical axis). The contours are a crude estimate at best, however, they do provide a means of getting a first estimate of the wave coherence function between two locations. Fig. 7 is a plot of Eq. 10 for constant values of theta.

Fig. 8 shows four coherence plots from this experiment along with the estimate of coherence obtained from Eq. 10. The dashed portion of the estimate represents application of Eq. 10 outside the frequency range 0.08 - 0.16 hertz. The estimate for Run 8 is the product of the separate coherence functions determined for the primary and secondary wave directions. Eq. 10 is seen to reproduce a reasonable estimate for planning purposes.

The estimation technique was also applied to the data of Kuo, et al. (4) which were collected from a triangular array, 7 meters on a side, located in 15.5 meters depth. The estimate (see Fig. 9) is reasonable even well outside the frequency range used to establish the empirical constants. This is probably because of the close proximity of the gages.

DISCUSSION

An empirical equation for estimating wave coherence in terms of spatial separation has been formulated using a select portion of the original data set, and thus, the limits of applicability have been defined. Within the frequency range 0.08 - 0.16 hertz, the empirical equation can be expected to provide a fair estimate of wave coherence. At higher frequencies the coherence decreases more rapidly than Eq. 10 would predict. This indicates that the parameterization of frequency in terms of wavelength is incorrect at higher frequencies.

There was no clear difference in wave coherence between conditions representing swell and storm seas in the data analyzed. Swell waves can be expected to be longer-crested and less dispersive and thus less sensitive to spatial separation, but this was not clearly evident in the data. This observation may be a consequence of the finite depth influence, and the difference between sea and swell might become more apparent in deeper water. Since the results were obtained in a water depth of 17 meters, it is reasonable to expect some signature of the depth in the coherence function. The high coherence values observed in the frequency range 0.08 - 0.10 hertz are quite possibly

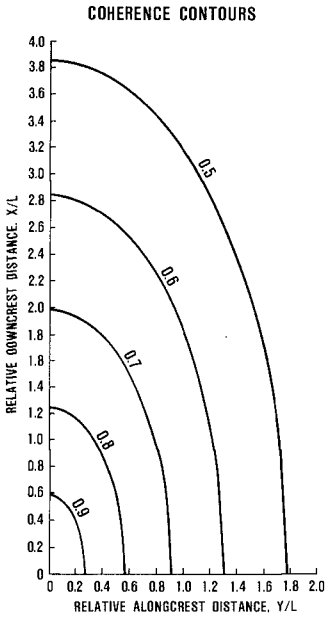


Figure 6. Wave Coherence Contours

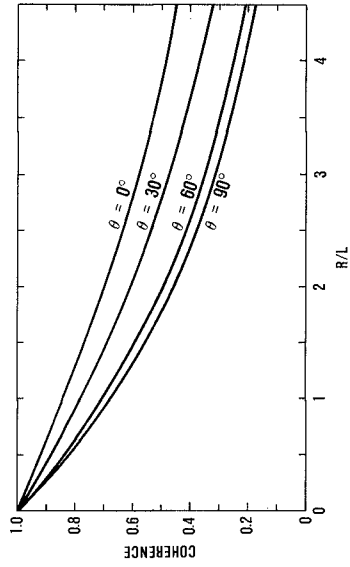


Figure 7. Coherence Curves of R/L Versus θ

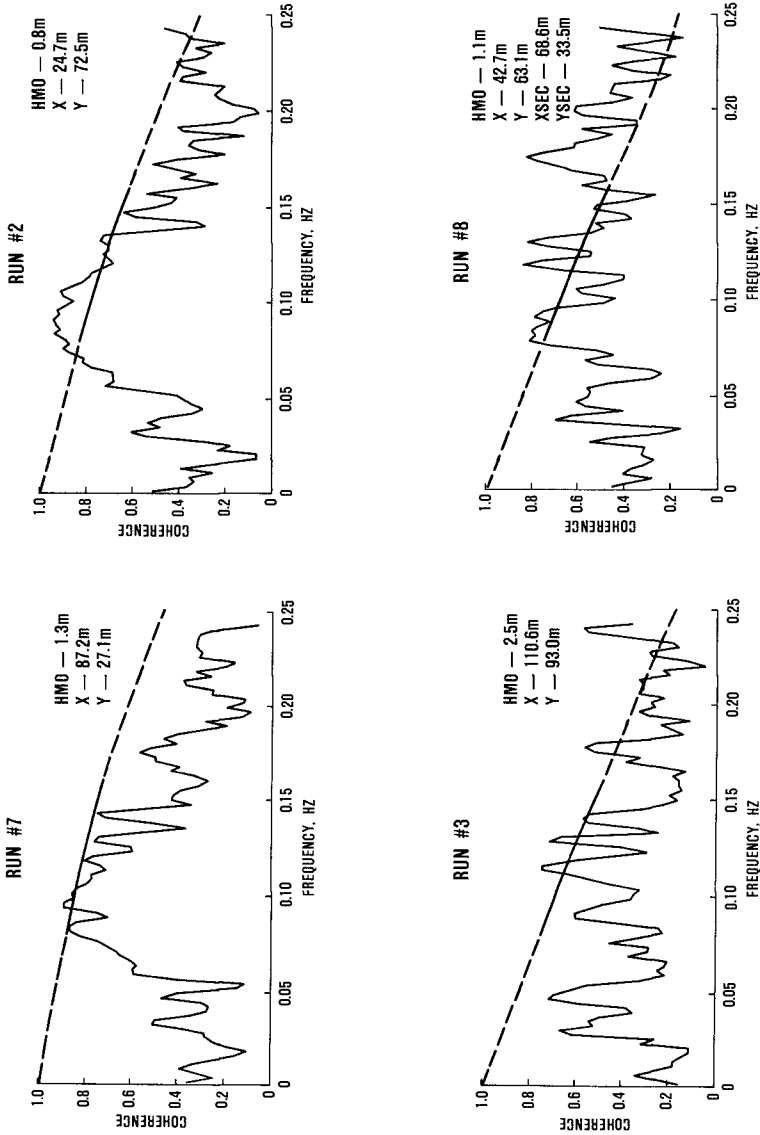


Figure 8. Coherence Estimates (This Experiment)

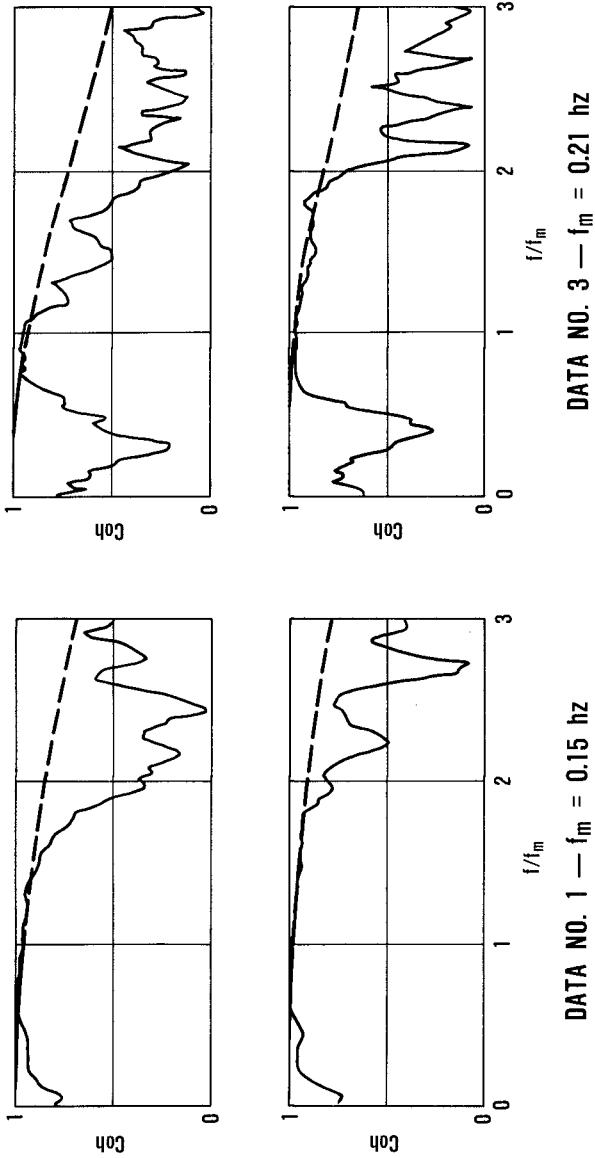


Figure 9. Coherence Estimates (Kuo, et al. Data)

related to the fact that waves at these frequencies have been rendered less dispersive by the finite depth. The observed decrease in coherence values at frequencies less than about 0.07 hertz may well be due to the minuscule amounts of energy at these low frequencies.

It must be emphasized that the equation for estimating wave coherence was obtained from data gathered in a water depth of 17 meters. It is expected that Eq. 10 could be applied at other water depths because of the nondimensionalizing by wavelength, however, more data are needed to support this generalization.

One interesting observation comes from comparing the theoretical wave coherence plots presented by Georgiadis and Hartz (2) with the empirical result given by Fig. 7. The theoretical coherence curves were obtained by assuming a JONSWAP spectrum in conjunction with selected directional spreading functions, and the results assume that the coherence function between two positions is strictly determined by the directional spreading. The theoretical curve which best follows the down-crest (0 degree) curve on Fig. 7 turns out to be the one found for a cosine to the sixth power. However, the corresponding theoretical curve for the along-crest direction (90 degrees) drops off to zero coherence before the value of R/L reaches 1.0. This is not the case for the empirical representation of the field data, as seen in Fig. 7. Thus, the along-crest coherence in shallow water is much better than predicted from the stated theoretical considerations. This could once again be a depth influence and possibly an indication that energy and directional spreading are not completely uncoupled in finite depth water.

Finally, the empirical equation presented for estimating the wave coherence function between two spatial locations should be used primarily as a planning tool due to the considerable variation present in the observed values. Attempts to use Eq. 10 to remove the effects of wave coherence from a system response might not be satisfactory in many cases. If the wave coherence between two positions is required during the course of an experiment, it is advisable to measure this coherence directly, using Eq. 10 as a planning guide.

SUMMARY

The Coastal Engineering Research Center has collected wave data from a closely spaced array of five wave gages at the Field Research Facility at Duck, North Carolina. The objective was to examine the spatial variability of the wave field in terms of the wave coherence function for a variety of incident wave conditions.

Qualitatively, the coherence function appears relatively independent of the shape of the spectrum, the spectral energy content, and the location of the spectral peak frequency for the range of conditions examined. The finite water depth at the site appears to render the lower fre-

quency waves less dispersive, and hence, more coherent so long as sufficient energy is present at those frequencies. The most apparent influence on the coherence is the spatial separation, and this effect was empirically quantified in terms of the relative wavelength. The resulting equation can be used to estimate the wave coherence function in finite depth water, but the uncertainty involved is substantial. A reasonable estimate is provided in the region between 0.08 - 0.16 hertz, but coherence is overestimated at higher frequencies. Consequently, these results are more suited for planning considerations.

ACKNOWLEDGMENTS

The research results contained in this paper were sponsored by the Naval Civil Engineering Laboratory. Field data collection was performed by the staff of the Field Research Facility. Permission to publish these findings was granted by the Naval Civil Engineering Laboratory and by the U.S. Army Chief of Engineers.

APPENDIX.—REFERENCES

1. BRIGGS, M.J., "Multichannel Maximum Entropy Method of Spectral Analysis Applied to Offshore Structures," WHOI-81-69, Woods Hole Oceanographic Institution, Woods Hole, Massachusetts, August 1981.
2. GEORGIADIS, C., and HARTZ, B.J., "Wave Coherence Along Continuous Structures For Directional Spectral Models," STF71 A82004, The Foundation of Scientific and Industrial Research at the Norwegian Institute of Technology, Trondheim, Norway, March 1982.
3. HUGHES, S.A., "Spatial Variability in the Nearshore Wavefield," Misc. Paper CERC-84-7, U.S. Army Engineer Waterways Experiment Station, Coastal Engineering Research Center, Vicksburg, Mississippi, 1984.
4. KUO, Y., MITSUYASU, H., and MASUDA, A., "Experimental Study on the Phase Velocity of Wind Waves, Part 2: Ocean Waves," Reports of Research Institute for Applied Mechanics, Vol. XXVII, No. 84, September 1979.
5. MATTIE, M.G., and HARRIS, D.L., "A System for Using Radar to Record Wave Direction," TR 79-1, U.S. Army, Corps of Engineers, Coastal Engineering Research Center, Ft. Belvoir, Virginia, September 1979.